STIMULATED RAMAN SCATTERING OF LIGHT BY ISOLATED TRANSPARENT DROPLETS

Yu.E. Geints, A.A. Zemlyanov, and E.K. Chistyakova

Institute of Atmospheric Optics,
Siberian Branch of the Russian Academy of Sciences, Tomsk
Received December 29, 1993

In this paper we present an overview of experimental data on stimulated Raman scattering (SRS) of light by weakly absorbing droplets of micrometer size. We also analyze the energy, temporal, and angular characteristics of the process. Physical prerequisites of the SRS effect in spherical particles and theoretical model of this process are discussed in the paper. We also consider in our overview the lasing and CARS effects in droplets and experimental techniques for studying the physicochemical properties of isolated droplets based on the SRS effect.

1. INTRODUCTION

The nonlinear optical resonant phenomena in the weakly absorbed liquid (stimulated Raman scattering (SRS), coherent anti–Stokes Raman scattering (CARS), coherent Raman mixing (CRM), and lasing) are discussed in the scientific literature for a long time. However, it have been found only at the recent time that these phenomena have the distinctive features for a liquid being in the disperse state (see Refs. 1–5 and 12–36). This applies to both spatiotemporal structure of a scattering signal (a peak spectrum within the Raman contour, delay of the scattered signal relative to a pump pulse)[12–20] and the threshold characteristics (the significant reduction of the SRS thresholds in droplets by comparison with that in a solid medium).[3]

A basic prerequisite for appearing resonant nonlinear optical phenomena in microns is occurrence of resonances of internal optical field (or the morphology–dependent resonances (MDRs)).[1,6–11] These resonances are visible at specific values of the particle diffraction parameter $\rho = 2\pi a/\lambda$, $\rho \gg 1$ (where a is the droplet radius, λ is the laser radiation wavelength) and characterized by the order and number of mode of partial electromagnetic wave forming the resonance. Resonances can be rather narrow with the quality factor $Q \geq 10^{20}$ for a homogeneous transparent spherical droplet. In practice Q achieves, as a rule, values $\sim 10^6$–10^8 (see Ref. 3). It is associated with both a nonzero absorption of a liquid and deviation of a droplet form from the ideal sphere due to capillary oscillations.

It is necessary to point out that although the qualitative pattern of process of the stimulated light scattering by microns can be considered as more or less understandable, the theoretical models describing such process are lacking. The vast majority of papers discussing these problems are the experimental investigations that is due to the awkward mathematical apparatus of Mie theory requiring performance of numerical calculation to obtain the concrete results, except for the novelty of this line of inquiry.

The present paper is review of the available experimental data on the SRS process within micron–size droplets that we have performed to systematize the results and reveal the regularity in the SRS process in spherical particles.

2. MORPHOLOGY–DEPENDENT RESONANCES IN WEAKLY ABSORBING DROPLETS

As is known from the quantum standpoint, the phenomenon of the Raman scattering is that one photon of incident light with the energy $\hbar\omega$ ($\hbar$ is the Plunk constant, ω is the radiation frequency) is absorbed by a molecule, and an another photon with energy $\hbar\omega'$ is emitted. Energy equal to $\hbar(\omega - \omega')$ is absorbed by a material, hence the own molecular oscillations are excited with the frequency $\Delta\omega$. The SRS appears only at the sufficiently high intensity of insident light. At low intensity spontaneous Raman scattering takes place, when thermal oscillations of molecules occur at random (noncoherently). In this case, intensity of scattered light is low (in 1 cm^3 there are $10^{-8} - 10^{-6}$ of the incident light intensity[28]) and its frequency ω' differs from the that of incident light by the value $\Delta\omega$ equal to the oscillation frequency of microns. At the very high intensity of incident light the nonlinear effects occur in a medium. Not only forces with frequencies of incident ω and scattered ω' radiation act on the microns, but also the force acts with the difference frequency $\Delta\omega$, i.e. with the frequency of the free micron oscillations that results in the resonant excitation of oscillations.

Excitation of intramolecular oscillations at the SRS occurs in that cases when the SRS takes place in a material at the state close to equilibrium. Therewith the frequency ω' of scattered light is less than the frequency of the incident radiation $\omega' = \omega - \Delta\omega$ (the Stokes process). At the stimulated light scattering not only excitation of the microns motion is possible but also its suppression if the initial state of the material is not equilibrium one and $\omega' = \omega + \Delta\omega$ (the anti–Stokes process).

It is known from the theory of diffraction of electromagnetic wave on the dielectric sphere (the Mie theory) that, when $\rho \gg 1$, its internal optical field is characterized by existence of the multitude of peaks with the sharp intensity difference $\sim 10 - 100$ times.[25] Therewith maximum values of internal optical field are achieved near the droplet surface. However, as investigations have shown, the internal optical field can be multiply amplified, particularly near the maximums (by $10^4 - 10^6$ times) at fixed values of the droplet

0235-6880/94/07 488-07 $02.00

radius.[6–8] Such effect is named as morphology–dependent resonances (MDRs) and considered as free oscillation (resonant) modes of the droplet, or spherical resonator. The existence of such resonances, which inmediately follows from the Mie theory, has been found at first in experiment by the presence of peaks in a scattered signal.[7]

We write using designations from Ref. 25 the components of electromagnetic field within a homogeneous spherical particle in the form

$$E_r = \frac{E_0 \cos\varphi}{k_i^2 r^2} \sum_{n=1}^{\infty} c_n\, n(n+1)\, \Psi_n(k_i r)\, Q_n(\theta) \sin\theta;$$

$$E_\theta = \frac{E_0 \cos\varphi}{k_i r} \sum_{n=1}^{\infty} \{c_n\, \Psi_n'(k_i r)\, S_n(\theta) + i\, b_n\, \Psi_n(k_i r)\, Q_n(\theta)\}; \quad (1)$$

$$E_\varphi = -\frac{E_0 \sin\varphi}{k_i r} \sum_{n=1}^{\infty} \{c_n\, \Psi_n'(k_i r)\, Q_n(\theta) + i\, b_n\, \Psi_n(k_i r)\, S_n(\theta)\};$$

$$H_r = -\frac{E_0 \sin\varphi}{k_i k_0 r^2} \sum_{n=1}^{\infty} b_n\, n(n+1)\, \Psi_n(k_i r)\, Q_n(\theta) \sin\theta;$$

$$H_\theta = -\frac{E_0 \sin\varphi}{k_0 r^2} \sum_{n=1}^{\infty} \{b_n\, \Psi_n'(k_i r)\, S_n(\theta) + i\, c_n\, \Psi_n(k_i r)\, Q_n(\theta)\}; \quad (2)$$

$$H_\varphi = -\frac{E_0 \cos\varphi}{k_0 r^2} \sum_{n=1}^{\infty} \{b_n\, \Psi_n'(k_i r)\, Q_n(\theta) + i\, c_n\, \Psi_n(k_i r)\, S_n(\theta)\}.$$

Here the primes mean the derivative with respect to the argument, presented in the parentheses; $k_i = 2\pi m_i/\lambda$ is the wave number; k_0 is that in a vacuum; r, θ, φ, are the spherical coordinates of a point within a particle; E_0 is the electric intensity in the incident wave; H is the magnetic intensity; and, c_n and b_n are the amplitudes of partial waves.

Degree of inhomogeneity of an internal optical field in a particle is characterized, as a rule, by the relation

$$B = \frac{E_r E_r^* + E_\theta E_\theta^* + E_\varphi E_\varphi^*}{E_0^2},$$

taking into account interaction of the incident wave with a material in the particle bulk (factor of inhomogeneity of an internal intensity).

It is seen from relations describing the electric E_i and magnetic H_i fields in a droplet that behavior of the internal electromagnetic field is completely determined by the amplitudes of partial waves c_n and b_n

$$c_n = i^n \frac{2n+1}{n(n+1)} \frac{m}{\xi_n(\rho)\, \Psi_n'(m\rho) - m\, \xi_n'(\rho)\, \Psi_n(m\rho)};$$

$$b_n = i^n \frac{2n+1}{n(n+1)} \frac{-m}{\xi_n'(\rho)\, \Psi_n(m\rho) - m\, \xi_n(\rho)\, \Psi_n'(m\rho)}. \quad (3)$$

MDRs are connected with zeros of denominators in the relations for c_n and b_n, and its locations are determined only by values $m = (m_i/m_0)$ and ρ, where $m_i = n_i + i\kappa_i$ is the complex refractive index of the droplet material, m_0 is that for a medium. Thus, it is necessary to determine location of zeros along the scale ρ in the denominators of Eq. (3).[23]

In general terms an infinite set of values of the diffraction parameters $\rho_n^1 < \rho_n^2 < \rho_n^3 < \rho_n^l$ exists for any fixed value of n such that c_n or b_n is maximum (MDRs). MDRs for the coefficients c_n^l correspond to resonant TH_n^l partial waves and for b_n^l to TE_n^l. Investigations[21–22] have shown that

1) $\rho_n^l \sim n$;

2) the relative height of a resonant peak for the given mode decreases whereas width increases with growth of the order l.

3) the inverse process occurs at fixed l and increasing n;

4) the distance between sequent MDRs (along the axis ρ) between b_n^1 and b_{n+1}^l and c_n^1 and c_{n+1}^l under condition $\rho \gg 1$, $n \sim \rho$, and $m\rho \geq n$ can be approximately calculated from the expression presented in Ref. 11

$$\Delta\rho \cong \arctan\left[\sqrt{\frac{(|m|^2 - 1)}{|m|}}\right] \frac{1}{\sqrt{|m|^2 - 1}}$$

and is independent of neither ρ nor n;

5) at $\rho > 1$ no MDRs is observed. This is to say that occurrence of MDRs in spherical particles is due to summation of the high frequency components (with large n), i.e., symmetry of a droplet, rather than interferation of partial waves inside a droplet and thus resonances are not observed for non–spherical particles;

6) the resonant structure of field within a droplet depends on the order l. It has been established in Ref. 6 that TE_n^l resonant mode has l peaks between a surface and center of a droplet (if consider the main cross section) and the TH_n^l mode has $(l+1)$ peaks (only strongest resonances are considered). For cylindric particles (for both TE_n^l and TH_n^l waves) l high peaks is observed.

For large droplets with $\rho \sim n \gg 1$ equations (1) for components of the internal electromagnetic field is essentially simplified, that allows the get asymptotical expressions for the basic MDRs characteristics[37] to be obtained

for ρ_n^l position (along the ρ axis)

$$n_i \rho_n^l = \nu + 2^{-1/3} \alpha_l \nu^{1/3} - \frac{P}{(n_i^2 - 1)^{1/2}} + \left(\frac{3}{10} 2^{-2/3}\right) a_l^2 \nu^{-1/3} - \frac{2^{-1/3} P (n_i^2 - 2P^{2/3})}{(n_i^2 - 1)^{3/2}} \alpha_l \nu^{-2/3} + O(\nu^{-1}),$$

$P = n_i$ for TE and $P = 1/n_i$ for TH;

for the halfwidth Γ_n^l

$\Gamma_n^l = 1 / N_1 \xi^2(\rho_n^l)$, $N_1 = n_i^2 - 1$ for TE,

$N_1 = (n_i^2 - 1)[\mu^2 + \mu^2/(n^2 - 1)]$ for TH;

for the spacing between resonances $\Delta\rho_n^l$

$$n_i \Delta\rho_n^l = 1 + \frac{2^{1/3}}{3} \alpha_l \nu^{-2/3} - \frac{2^{-2/3}}{10} \alpha_l^2 \nu^{-4/3} + \left[\frac{2^{1/3}}{3} \frac{P(n_i^2 - 2P^{2/3})}{(n_i^2 - 1)^{2/3}} - \frac{2^{-1/3}}{9}\right] \alpha_l \nu^{-5/3} + O(\nu^{-2}),$$

where the coefficient $v = n + 1/2$; $\mu = \nu/\rho_n^l$; and, α_l is the ith root of the function $Ai(-z)$.

Presented above fomulas follow from asymptotic behavior of the Bessel functions ξ_n and ψ_n and so their accuracy is rather high (difference from exact values calculated by the Mie fomulas is less than 0.1%) and increases with the increase of the order n. Other approximative fomulas for ρ_n^l, Γ_n^l, and $\Delta\rho_n^l$ calculation are known, for example, fomulas derived in Ref. 38. However, they have the lower accuracy.

Let us dwell on the influence of refractive index of a droplet material κ on the MDRs. The increase of κ ($\kappa \ll 1$) results, first of all, in the reduce of intensity of highest near–surface peaks and in the quenching of resonances of the highest orders (the large l, i.e., the spectrum waviness disappears). It was noticed[16] that the absorption practically does not result in shifts of the MDRs peaks along the scale ρ. Moreover, even though a particle is nonhomogeneous, for example, solid particles of the strongly absorbing material are added in transparent liquid (hematite in glycerin[16]), the MDRs spectrum is close to the spectrum for the homogeneous droplet with some effective value κ.

Let us consider the physical mechanism of the SRS occurrence in a spherical droplet. The theoretical model of the SRS generation by micron droplets is based on the MDRs occurence in weakly absorbing droplets with $\rho \gg 1$. As was mentioned, the incident field is mainly focused by the illuminated face into small region just near the shade droplet surface (see Fig. 1).

The input resonance is achieved when wavelength of the incident radiation λ_L is tuned to one of MDRs. In this case the optical intensity in the droplet increases hundred times, essentially near the surface. The output resonance is achieved when one of the second emission (for example, the Raman scattering or fluorescence) wavelengths λ_S is coincident with some MDRs. For such wavelength a drop can be considered as an optical resonator with its own resonant mode. Loses in such resonator are due to both absorption of a droplet material and partial output of radiation through the droplet surface.

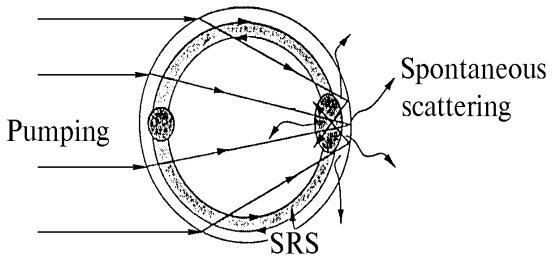

FIG. 1. Scheme of rays of the incident beam and spatial distribution of pumping fields and SRS within droplet.[17]

It is obviously that the spontaneous Raman scattering (RS) occurs throughout a drop, but it undergoes the maximum amplification of intensity near the focal volume of incident radiation. Portion of waves from the spontaneous RS spectrum leaves a drop, another portion propagates along the spherical surface in a curcle owing the complete internal reflection (Fig. 1). These waves both attenuate and amplify on the way. If the condition of the output resonance is satisfied for some λ_S then amplification begins to dominate over the absorption, and stimulated scattering occurs at some time. If consider a drop as spherical resonator then the SRS field can be treated as a standing wave formed as a result of superposition of electromagnetic waves propagating in opposite directions along the spherical droplet surface.

Thus, a necessary condition for the SRS occurence in the spherical weakly absorbing droplet is the fulfilment of the condition of the output (with λ_S) resonance. Therewith the corresponding resonance should be of sufficiently high quality factor (or Q). The situation, when both the input and output resonances occur in a particle, is unlikely to be realized. In this case, obviously, the significant reduce of the energetic SRS threshold due to amplification of the pumping intensity within a drop[3] is to be expected.

3. STIMULATED FLOURESCENCE OR LASING IN TRANSPARENT DROPLETS. MULTIORDER SRS

This phenomenon is reffered to as lasing by analogy with generation in dye lasers. Molecules of the optically active dye (for example, rhodamine 6G or coumarin 481) are put in transparent droplets, which, as shown above, can be considered as spherical resonators. When droplets are irradiated by laser radiation in the specified spectrum range, molecules begin to fluoresce. Otherwise the mechanism of arising stimulated fluorence is similar to the SRS with the only difference that there are many different MDRs with different wavelengths within the spontaneous fluorescence spectrum, because it is sufficiently wide (Fig. 2). In Fig. 2 fluorescence and absorption of a volume liquid are shown. Lasing is unstable in the frequency range A. In the range B the sequence of quasi–periodic peaks is observed. SRS was registred at $\lambda = 630$ nm. In dye–doped droplets the SRS can arise in a basic liquid also, but this effect is far weaker than fluorescence of dye–stuff molecules and quenched by it at the initial stage of the process. However, the SRS peaks in a basic liquid can be detected experimentally[31] after the dye–stuff molecules de–excitation.

The first Stokes component of SRS occuring within the droplet can serve as pumping one for the second Stokes component,[19] if it is of siquificantly high intensity. Therewith, naturally, the filfilment of conditions for existance of the input and output resonances in a droplet respectively for the 1st and 2nd orders of the Stokes components is necessary. In the experiments the SRS emission was observed up to the 14-th order (in CCL_4 droplets[19]). The characteristic feature of multiorder SRS within droplets as distinct from an optical cell is high intensity relative to the first–order Stokes. It is due to the pumping length that is equal approximately to $2\pi a_0$ for the second–order Stokes peak pumped by the first–order Stokes peak, while the pumping length for the first–order Stokes peak is only part of the droplet radius (a focal volume), because it is pumped by incident radiation.

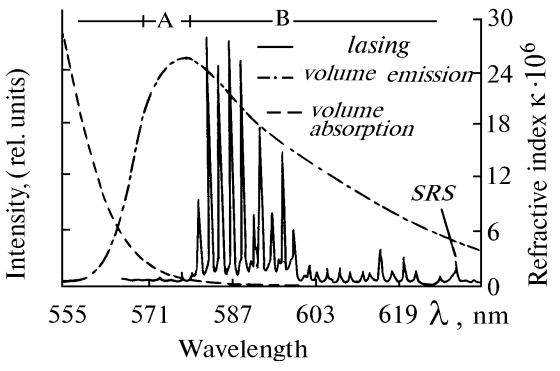

FIG. 2. Typical emission spectra for standard 12–μm *radius ethanol droplet mixed with rhodamine 6G.*[30]

Thus, the SRS spectrum (or lasing one) is defined as sequence of equidistant peaks corresponding to Stokes components of different orders: $\omega_{iS} = \omega_L + i\omega_S$, where ω_S is the frequency of the first Stokes line (i is the integer number, $i > 0$). If the droplet liquid is a mixture or a solt solution the spectrum is already more complicated. It is superposition of two or more spectra from the basic liquid and from soluble materials.[29] In Fig. 3 typical SRS spectra in the CCl_4 droplets and optical cell are presented together with the position of three basic Stokes components of CCl_4 with frequencies ν_1 =459, ν_2 = 218, and ν_4 = 314 cm^{-1}; [n00] means nth order of Stokes emission with the frequency shift ν_1. In the experiments Q–switched Nd:YAG laser was used, its radiation (the second harmonic output λ = 532 μm) was focused into the droplet stream. Average exitance at the focal range was of ~ 1 GW/cm^2. The SRS signal was detected by an optical multichannel analyzer. The elastic scattering background was blocked by color filters placed in front of the detector.

4. COHERENT ANTI–STOKES RAMAN SCATTERING (CARS)

Phenomena of the coherent anti–Stokes Raman scattering (below, CARS) require the fulfilment of the phase synchronism condition, as distinct from the Stokes scattering. Therewith as follows from experiments performed in Refs. 13 and 31, existence of the input resonance for the incident and (or) Stokes waves leaves the CARS intensity in droplets practically unaffected. This says that the condition of phase synchronism cannot be satisfied along a droplet circle. It can be satisfied only in the direction of propagation of pumping ω_L and Stokes ω_S wavesand consists in the distinct relation between the directions of the pumping wave vector $\mathbf{k}_L$ and Stokes wave vector $\mathbf{k}_S$, when conditions for interaction of these waves are most favour.

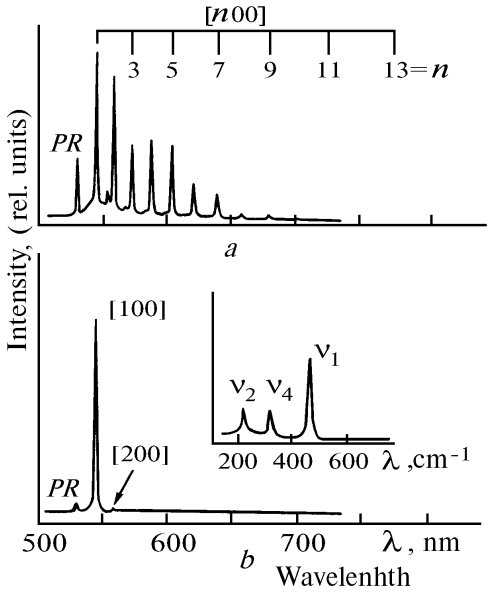

FIG. 3. Single–pulse SRS spectrum from a CCl_4 *droplets* 35 μm *in radius (a) and* CCl_4 *in an* 11–cm *cell*[19] *(b). The inset shows the spontaneous Raman scattering (RS). PR is the pumping radiation.*

Because the Stokes field occuring at Raman scattering is distributed along the outside droplet surface and condition of the phase synchronism with the pumping field fails, it is possible to obtain CARS signal in the experiment only in simultaneous illuminating of a droplet by pumping wave (ω_L) and radiation with the frequency equal to that of Stokes emission ω_S (Fig. 4).

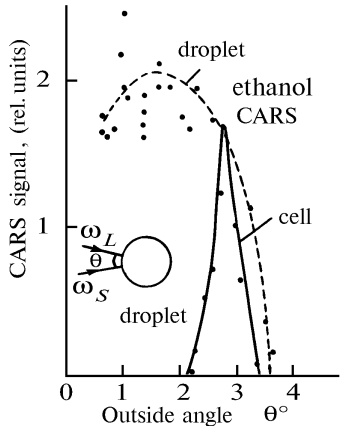

FIG. 4. CARS signal from ethanol droplets and ethanol in the cell as a function of the outside angle θ *between two input beams with* ω_L *and* ω_S *(Ref.* 13*).*

Experiments[13] have shown that maximum CARS signal in the ethanol droplets is observed when the outside angle between ω_L and ω_S is $\theta \approx 1.5°$. At the same time, the anglular dependence of the CARS amplitude in the optical cell has maximum at $\theta \approx 2.8°$, it is symmetric and more narrow than in the case of CARS from droplets. Pointed above distintions can be explained by features of the internal distribution of fields ω_L and ω_S.

The existence of spherical surface in a droplet makes the added shift into wave vectors $\mathbf{k} \to \mathbf{k}_i + \Delta\mathbf{k}$, i.e., θ is broadened symmetrically in both sides from $\theta \approx 2.8°$ for plane waves. And the angle of the phase synchronism shifts in the direction of smaller angles because the overlap of focal volumes of waves with ω_L and ω_S interaction is maximum at collinear geometry, i.e., at $\theta = 0°$.

Thus, the presence of phase synchronism condition for CARS indicates that CARS process (as any process of the coherent wave shift) occurs mainly within the focal volume in a droplet, where two waves with ω_L and ω_S are overlapped. Anti–Stokes wave weakly depends on the MDRs existence and does not result in the characteristic resonant structure of CARS spectrum.

5. TEMPORAL SRS CHARACTERISTICS IN PARTICLES

One of basic distinctions of SRS process in droplets from that in continuum is the occurence of temporal delay of the SRS by comparison with beginning of pumping–pulse irradition (see Refs.10, 15, 30, and 33). Because the SRS mechanism is similar both in the first and second cases the cause of delay Δt should obviously be found if to consider features of the SRS within small bulk. In the framework of given model of the SRS process the time delay Δt follows from the finitness of the time of formation of the SRS signal. That is just as appearance of stimulated emission in

a laser or, more exactly, in an optical resonator, so the light wave must pass the certain number of the passages from one mirror to another one (in a droplet it must move in a circle along the surface where the total internal reflection from surface acts as mirror) to form the siqnificantly power radiation which could be recorded experimentally.

Typical values of Δt fall in the interval $1 \le \Delta t \le 10$ ns in the experiments with micron–size droplets,[30] and they are practically independent on the droplet size. It indicates that MDRs with similar (in order of magnitude) Q–factor of $10^5 - 10^6$ play the basic role in the SRS formation.

A completely different type of situation occurs in varing the pumping intensity I_L. The time delay noticeably depends on I_L, therewith Δt increases at the I_L reduction and vice versa.[33] This situation will be discussed of below.

In experiments described in Refs. 15 and 33 the time required for initiation of multiorder SRS was studied (see Fig. 5). It turned out that delay of, for example, the second Stokes component is $\Delta t_2 < \Delta t$ under the same conditions. This fact is explained by the different generation mechanisms for the first Stokes component and higher–order ones.

The first Stokes component is formed from the spontaneous RS field or background, E_S that is excited by incident field E_0 in focal volume

$$\partial E_S / \partial r \sim \chi^{(3)} E_0 E_0^* E_S ,$$

where $\chi^{(3)}$ is the third moment (in the expansion over E_0) of the electric susceptibility of the liquid, r is the distance passed by the wave E_0 in a circle along the droplet surface. The formation of the second Stokes order (E_{2S}) is due to the process of parametric (fourth–wave) wave mixing rather than spontaneous RS (E_S)

$$E_{2S} / \partial r \sim \chi^{(3)} E_0 E_0^* E_{2S} + \chi^{(3)} E_0 E_0^* E_S \exp(i \Delta k r). \qquad (4)$$

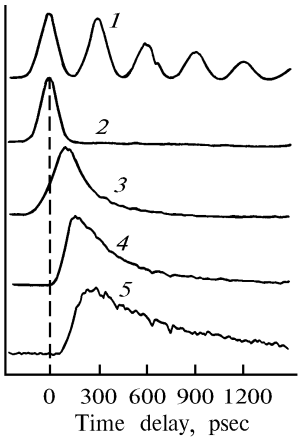

FIG. 5. The time profiles of the following signals from ethanol droplets (a_0 = 45 μm)[15]: at the output of Farby–Perot interferometer (1); input radiation (2); elastic scattering from a droplet (3); first–order Stokes component of SRS (4); and, second–order Stokes component of SRS (5).

In the formula (4) $\Delta k = k_{2S} + k_0 - 2k_S$ accounts for the condition of the phase synchronism for the wave E_{2S}. Just the second term on the right–hand side of Eq. (4) provides the fast growth of E_{2S} at the initial stage of formation of the 2nd Stokes component. At $r > l_{coh} = \pi / \Delta k$ (where l_{coh} is the coherent length) the exponent in the right–hand side of Eq. (4) quenchs the parametric amplification (the second term), but the first term, becomes valid because the field E_{2S} is already significantly strong, proviging the futher exponent growth of the second Stokes component.

In particular, it follows from represented above expressions that the increase of pumping intensity ($E_0 E_0^*$) results in more fast growth of intensity of both the first and the second Stokes components and, consequently, reduction of Δt and Δt_2.

Duration of the SRS signal τ also varies with varing I_L, and just τ growths with the reduce of I_L.[13] Besides, at the SRS exciting by supershort pulses ($\tau_p \sim 100$ ps) the SRS radiation is observed after termination of pumping pulse too, and τ / τ_p is ~ 100–500. Duration of the SRS signal is directly associated with Q–factor of the MDR responsible for the given resonance signal, because the de–excitation time $\tau \cong Q / \omega_S$. It is obviously that the noticed dependence of τ on I_L can be explained by sacrifice of resonant properties of a droplet at the increase of pumping intensity because significantly strong SRS at the first–order Stokes components excites the second–order one and so on, and consequently the essential part of the basic mode energy is expanded for generation of the other modes.

6. APPLICATION OF NONLINEAR RESONANT PHENOMENA FOR MEASUREMENT OF MICROPHYSICAL DROPLET PARAMETERS

As follows from previous presentation, the spectrum position of resonant peaks in scattered signal from droplets is uniquely determined by the radius, form, and refractive index of the particle. Thus, any variation of a droplet radius (form) $\Delta a / a$ results in corresponding changes in position of resonant peaks ($\Delta\lambda / \lambda$): $(\Delta a / a) = \Delta\lambda / \lambda$. Reduction of a droplet radius results in the resonant spectrum shift in the direction of shorther waves and increase of that leads to the red–range shift.

At addition of the strongly fluorescent dye molecules in a droplet the similar peaks (MDRs) are observed in the lasing spectrum too. Because their intensity is essentially higher than SRS one hence it is more convenient to study the peak shifts in the fluorescence spectrum in the experiments.

This idea was realized in Ref. 18. The stream of high–monodispersed droplets, producted by a Berlung–Liu piezoelectric vibrating–orifice droplet generator emerged from the vertically directed nozzle and passed through the laser beam directed along the horizontal axis. Droplets ($a_0 \sim 30$ μm) were illuminated by the focused radiation of the N_2 laser, exciting the fluorescence in dye molecules (ethanol + coumarin 481). Fluorescence was recorded by a spectral device. While droplets were falling they evaporated and, concequently, the spectral position of resonance varied. So, the MDRs shift along a wavelength scale over $\Delta\lambda = 0.11$ μm corresponded to reduction of the droplet radius Δr by 0.71 μm.

This technique is taken to be used (among other factors) in investigations in evaporation rates of a fuel droplets to find out the theory of droplet interaction processes.

At the study of the droplet surface oscillation, they were irradiated by powerful Ar^+ laser, and the fluorescence was excited by the N_2 laser. The spherical oscillations of a droplet results in the shift of whole spectrum of the fluorescent resonances into either blue range (for an extended sphere) or red one (for collapsed sphere).

If to measure the oscillation frequency f_2 and the oscillation decay constant τ_2, the surface tension σ and kinematic viscosity ν_k of liquid can be calculated because

$$f_2^2 = 2\sigma/\pi^2 \rho_{lq} a^2 , \tau_2 = a^2/5 \nu_k ,$$

where ρ_{lq} is the liquid density.

Authors of Ref. 34 and 35 developed and realized experimentally the efficient algorithm for determing the droplet radius from measurements of the resonant spectrum from spherical liquid particles. The process is completely automated. The range of the resonant spectrum is recorded, figured, and then input into computer. Special program with block for the resonant peak identification forms the file containing the position and intensity of peaks that are compared then with corresponding portion of the reference file, calculated by the Mie theory for a various droplet radius until the achivement of required accuracy. The measuring accuracy of the radius a_0 by this technique is estimated by authors as $\varepsilon \approx 0.03$ %. It should be noted that *prior* to measurement the information about refractive index value is required.

The continuous evolution of this technique have been done in Ref. 36. The measurement accuracy have been enhanced in following way: first, significantly long spectrum range involving more than hundred resonant peaks can be analyzed, second, dispersion of refractive index caused by cooling of surface layer of a droplet at its evaporation and added radiative losses due to existence of microcomponents in a liquid were taken into account.

It is obviously that considered above algorithm is appropriate to single droplets or to the sream of high–monodispersed droplets and completely unsuitable for polydisperse system such as, for example, aerosols from sprays and atmospheric aerosols. Thus, another technique was suggested in Ref. 17, which idea is based on the dependence of the energetic threshold for stimulated emissions (SRS, lasing) on the droplet size. Actually, the more particle the higher Q – factor of MDRs, and the less losses of MDRs photons and consequently lower the pumping intensity requied to excite the stimulated emission. Thus, at fixed pumping level I_L the SRS signal can be recorded from droplets, which radius is more than some threshold one $a_0(I_L)$. At the known mass concentration of particles and the dependence $I_L(a)$ the histogram of counted aerosol concentration can be obtained.

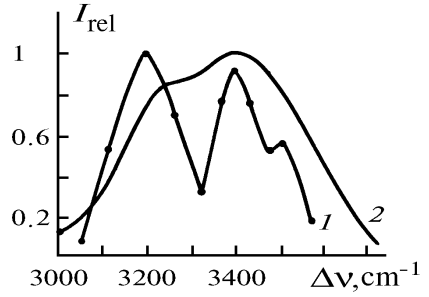

FIG. 6. The relative intensity distribution in spectra: SRS (1) and spontaneous RS[26] *(2).*

Experiments measuring the SRS from the water aerosol in the real atmosphere are of interest in our opinion. So, measurememts of a form, position , and width of the RS spectrum in the dense aqueoces hazes, fogs, and precipitations were carried out in Refs. 26, 27. The monostatic lidar with the second harmonic of Nd: YAG laser was used. The laser radiant flux was ~ 13 MW in a pulse (radiant exitance ~ 0.5 GW/cm^2). The radiation divergence on the level 0.8 was in order 0.1°. Signal was received from the path with length 1.5 km and initial delay 30 m corresponding to the lidar shadow zone. The signal was normalized to the RS line from the atmospheric N_2. The Stokes region of valence oscillations of a liquid water phase with the frequency shift ~ 3000 – 3800 cm^{-1} was studied. In Fig. 6 the distributions of relative intensity for the spontaneous RS from water and for SRS at remote sensing of aqueous aerosol in the atmosphere are presented.

It is seen from the figure that halfwidths of single lines in SRS spectrum are far smaller than that of corresponding line in the spontaneous scattering spectrum. Moreover, it was found that intensity relation for these lines as well as their center positions depend on microstructure and water concentration of aerosol. For example, when change over the sensing of fog to sensing of rain at fixed laser pumping power the intensity conversion in the Fermi doublet of the RS spectrum from the liquid was observed. This phenomena authors explain by the change of the opposite Fermi resonance sign at the increasing pumping power during the process of meeting SRS–amplification by the system of water droplets.

CONCLUSION

Thus, let us formulate briefly, the basic laws of the SRS process in transparent droplets. The SRS spectrum consists of the quiasiperiodic peaks within the spontaneous Raman profile. Each peak is associated with an particular free oscillating mode of the droplet–resonator (Fig. 7). The peak intensity depends on both the number of a resonant mode and its order. The greater a droplet radius, the higher the Q–factor of MDRs and more dense they are placed along the scale ρ and, consequently, more easily the emission threshold can be achieved. The growth of absorption coefficient of the droplet material results in the reduction of the SRS intensity. In this case the MDRs spectrum position is practically fixed.

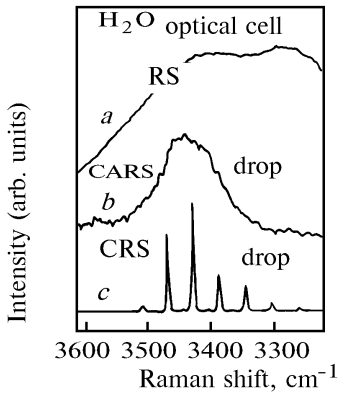

FIG. 7. Spectra:[33] *spontaneous Raman spectrum of* H_2O *in an 1–cm optical cell (a); CARS (b); and, SRS within* H_2O *droplets with* $a_0 \sim 30$ μm *(c).*

The SRS duration is proportional to the Q–factor of corresponding resonant mode determing the lifetime of the MDRs photons in a droplet. The SRS signal arises with some time delay relative to the begining of pumping pulse. It is due to required repeated multipassage of RS wave along the droplet surface to be of intensity significant for recording in the experiment. The delay value weakly depends on the droplet size and is determined mainly by the quantum output of the spontaneous Raman scattering of a liquid.

REFERENCES

1.R.G. Pinnick, A. Biswas, P. Chylek, and R.L. Armstrong, Opt. Lett. **13**, 494–496 (1988).
2. A. Biswas, H. Latifi, R.L. Armstrong, and R.G. Pinnick, Phys. Rev. A. **40**, No. 12, 7413–7416 (1989).
3. R.G. Pinnick, A. Biswas, J. Pendelton, and R.L. Armstrong, Appl. Opt. **31**, No. 3, 987–996 (1992).
4. J.–G. Xie, T.E. Ruekgauer, R.L. Armstrong, and R.G. Pinnick, Opt. Lett. **16**, No. 17, 1310–1312 (1991).
5. J.–G. Xie, T.E. Ruekgauer, R.L. Armstrong, and R.G. Pinnick, Opt. Lett. **16**, No. 23, 1817–1819 (1991).
6. P. Chylek, J.D. Pendelton, and R.G. Pinnick, Appl. Opt. **24**, No. 23, 3940–3942 (1985).
7. P. Chylek, J.T. Kiehl, and M.K.W. Ko, Appl. Opt. **17**, No. 19, 3019–3021 (1978).
8. P. Chylek, H.B. Lin, J.D. Eversole, and A.J. Campillio, Opt. Lett. **16**, No. 22, 1723–1725 (1991).
9. P. Chylek, D. Ngo, and R.G. Pinnick, J. Opt. Soc. Am. A. **20**, No. 10, 1803–1814 (1981).
10. P. Chylek, A. Biswas, R.G. Pinnick et al., Appl. Phys. Lett. **52**, No. 19, 1642–1644 (1988).
11. P. Chylek, J. Opt. Soc. Am. **66**, No. 3, 285–287 (1976).
12. S.–H. Qian, J.B. Snow, and R.K. Chang, Opt. Lett. **10**, No. 10, 499–501 (1985).
13. R.K. Chang, S.–X. Qian, and J. Eickmans in: *Proceeding of the Methods of Laser Spectroscopy Symposium,* Israel, (1985), pp. 1–10.
14. J.B. Snow, S.–X. Qian, and R.K. Chang, Opt. News. **12**, No. 5, 5–7 (1986).
15. J.H. Zhang, D.H. Leach, and R.K. Chang, Opt. Lett. **13**, No. 4, 270–272 (1988).
16. J.H. Zhang, G. Chen, and R.K. Chang, J.Opt. Soc. Am. B **7**, No. 1, 108–115 (1990).
17. A. Serpengurel, J. Swindal, and R.K. Chang, Appl. Opt. **31**, No. 18, 3543–3551 (1992).
18. H.–M. Tzeng, M.B. Long, R.K. Chang, and P.W. Barber, SPIE **573**, 80–83 (1985).
19. S.–X. Qian and R.K. Chang, Phys. Rev. Lett. 56, No. **9**, 926–929 (1986).
20. S.–X. Qian, J.B. Snow, H.–M. Tzeng, and R.K. Chang, Reprint Series **231**, 486–488 (1986).
21. G.J. Rosasco and H.S. Bennett, J. Opt. Soc. Am. **68**, No. 9, 1242–1250 (1978).
22. P.R. Conwell, P.W. Barber, and C.K. Rushforth, J. Opt. Soc. Am. **1**, No. 1, 62–66 (1984).
23. H.B. Lin, J.D. Eversole, and A.J. Campillo, Opt. Lett. **17**, No. 11, 828–830 (1992).
24. A. Ashkin and J.M. Dziedzic, Appl. Opt., **20**, No. 10, 1803–1814 (1981).
25. A.P. Prishivalko, *Optical and Thermal Fields within Light Scattering Particles* (Nauka i Technika, Minsk, 1983), 190 pp.
26. U.Kh. Kopvillem, O.A. Bukin, V.M. Chudnovskii, et. al. Opt. Spektrosk., **59**, No. 2, 306–309 (1985).
27. O.A. Bukin, U.Kn. Konvillem, C.Yu. Stolyarchuk, and V.A. Tyapkin. Zh. Prikl. Spektrosk. **38**, 778 (1983).
28. M.M. Suschinskii, *Stimulated Light Scattering* (Nauka, Moscow, 1985) 176 pp.
29. A. Biswas, R.L. Armstrong, and R.G. Pinnick, Opt. Lett. **15**, 1191–1193 (1990).
30. A. Biswas, H. Latifi, R.L. Armstrong, and R.G. Pinnick, Opt. Lett. **14**, 214–216 (1989).
31. H. Latifi, A. Biswas, R.L. Armstrong, and R.G. Pinnick, Appl. Opt. **29**, 5387–5392 (1990).
32. S.–X. Qian, J.B. Snow, and R.K. Chang, Opt. Lett. **10**, 499–501 (1985).
33. W.–F. Hsieh, H.–M. Tzeng, and R.K. Chang, Opt. Lett. **13**, 497–499 (1988).
34. P.R. Conwell, C.K. Rushforth, R.E. Barber, and S.C. Hill, J. Opt. Soc. Am. A **1**, No. 1, 1181–1187 (1984).
35. S.C. Hill, C.K. Rushforth, R.E. Barber, and P.R. Conwell. Appl. Opt. **24**, 2380–2390 (1985).
36. J.D. Eversole, H.–B. Lin, A.L. Huston, et. al. J. Opt. Soc. Am. B. **10**, 1955–1968 (1993).
37. C.C. Lam, P.T. Leung, and R. Yuong. J. Opt. Soc. Am. **9**, 1585–1592 (1992).
38. J.R. Probert–Zones. J. Opt. Soc. Am. A. **1**, 822–830 (1984).